CHIN. PHYS. LETT. Vol. 36, No. 6 (2019) 068501

Silicon on Insulator with Highly Uniform Top Si Fabricated by H/He Coimplantation *

Xin Su(苏鑫)[1,2], Nan Gao(高楠)[1,2], Meng Chen(陈猛)[3], Hong-Tao Xu(徐洪涛)[3], Xing Wei(魏星)[1,2,3**], Zeng-Feng Di(狄增峰)[1,2**]

[1]*State Key Laboratory of Functional Materials for Informatics, Shanghai Institute of Microsystem and Information Technology, Chinese Academy of Sciences, Shanghai 200050*
[2]*University of Chinese Academy of Sciences, Beijing 100049*
[3]*Shanghai Simgui Technology Co., Ltd., Shanghai 201815*

(Received 11 February 2019)

Silicon on insulator with highly uniform top Si is fabricated by co-implantation of H^+ and He^+ ions. Compared with the conventional ion-slicing process with H implantation only, the co-implanted specimens whose He depth is deeper than H profile have the top Si layer with better uniformity after splitting. In addition, the splitting occurs at the position that the maximum concentration peak of H overlaps with the secondary concentration peak of He after annealing. It is suggested that the H/He co-implantation technology is a promising approach for fabricating fully depleted silicon on insulator.

PACS: 85.40.Ry, 81.20.−n, 81.05.Cy DOI: 10.1088/0256-307X/36/6/068501

Ion-slicing technology has been successfully applied to realize the mass production of silicon-on-insulator (SOI) wafers.[1] Initially, to achieve successful layer transfer, the sufficient dose of hydrogen ions in the range of 3×10^{16}–$1\times10^{17}\,\mathrm{cm}^{-2}$ is required.[1–3] Therefore, for the economical fabrication of SOI wafers, ion-slicing technology based on H/He co-implantation is proposed due to the effective reduction of total dose.[4,5] Previous works have concluded that hydrogen atoms in silicon chemically interact with the implantation-induced damages which eventually form the H-terminated platelets or H-passivated micro-cracks. Under the following thermal process, partial H atoms detrapping from the complexes would form hydrogen gas to pressurize the platelets, which eventually implements the layer transfer. With the introduction of He, He atoms are free from the chemical interaction and possess high diffusivity in silicon. During annealing, He atoms readily diffuse into the H-terminated platelets to facilitate the pressurization process.[6,7] More recent works on co-implantation mainly focused on the implantation sequences,[8–11] thermal evolution of blisters,[12,13] platelets and complexes[11] and the relative depth distributions of H/He at low energies ($<$ 20 keV).[12] However, the influence of H/He co-implantation on the transferred silicon film thickness uniformity is seldom reported. As the requirement of silicon film thickness uniformity has reached ±5 Å for the fabrication of FD-SOI,[14] it is of great significance to explore a layer transfer method to achieve highly uniform top silicon.

In this Letter, an efficient layer transfer approach has been demonstrated by co-implantation of H^+ and He^+ ions sequentially at room temperature. Compared with hydrogen alone, it is worth noting that better top silicon uniformity after splitting can be achieved by co-implantation. When the distribution of He depth is deeper than hydrogen, the optimal uniformity can be realized.

The 8-inch (001) Si wafers covered by a 27-nm-thick thermal SiO_2 layer were implanted at room temperature by H^+, or H^+ then He^+ ions (thereafter referenced as the H-alone, or co-implanted samples, respectively). The thickness uniformity of the SiO_2 layer is ±1 Å. The co-implanted wafers were subjected to the same doses of H and He, each one of $1\times10^{16}\,\mathrm{cm}^{-2}$. H^+ ions were implanted at 18 keV. He^+ ions were implanted at different energies in the range from 30 to 45 keV, which ensures the He concentration peak largely overlaps or locates deeper than the H concentration peak. Thereafter, the co-implanted sample with 30 keV He implantation energy is referenced as S30, and the one with 45 keV He implantation energy is referenced as S45. For the H-alone samples, its implanted energy was 18 keV with the dose of $6\times10^{16}\,\mathrm{cm}^{-2}$. After the implantation, all wafers were annealed at 300℃ for 3 min and 500℃ for 30 min under nitrogen gas in a conventional furnace. The nominal H depth distribution was calculated by SRIM.[15] In addition, H and He depth-distributions were measured by secondary ion mass spectroscopy (SIMS) after the removal of the oxide layer. The blistering phenomena on the wafer surface were studied by scanning electron microscopy (SEM) and atomic force microscopy (AFM). Raman spectroscopy was

*Supported by the National Natural Science Foundation of China under Grant No 61674159, the Program of National Science and Technology Major Project under Grant No 2016ZX02301003, the Shanghai Academic/Technology Research Leader under Grant Nos 16XD1404200 and 17XD1424500, the Key Research Project of Frontier Science of Chinese Academy of Sciences under Grant No QYZDB-SSW-JSC021, and the Strategic Priority Research Program (B) of the Chinese Academy of Sciences under Grant No XDB30030000.

**Corresponding author. Email: xwei@mail.sim.ac.cn; zfdi@mail.sim.ac.cn

© 2019 Chinese Physical Society and IOP Publishing Ltd

used to characterize the various H-related complexes in the H-implanted zone. Cross-sectional transmission electron microscopy (XTEM) was used to examine the platelets, micro-cracks, damage layers formed in H-implanted zone after the thermal annealing. After splitting, the transferred layer thicknesses were characterized by spectroscopic ellipsometry (SE) and XTEM.

Figure 1(a) shows the thickness uniformity of the transferred Si layer. For H-alone wafer, the mean range is about 10.3 Å. However, it reduces to about 8.7 Å and 6.4 Å for the co-implanted wafers S30 and S45, respectively. It can be clearly seen that the co-implantation wafers can achieve a better uniformity. In addition, for the co-implantation samples, the uniformity of the transferred Si layer is closely related to the implantation energy of He, and the proper He energy to ensure the separation between H and He distributions is expected to achieve a better uniformity.

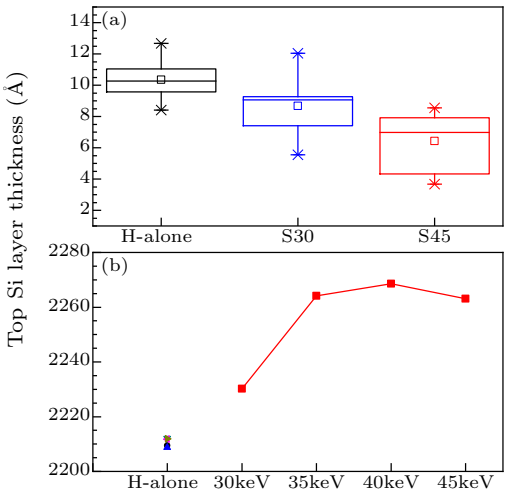

Fig. 1. Spectroscopic ellipsometry measurements of H-alone and co-implanted wafers. (a) The transferred Si layer thickness uniformity. (b) The transferred Si layer thickness. The energies on the horizontal axis in (b) represent the He^+ ion implantation energy.

The transferred Si film thicknesses are shown in Fig. 1(b). The mean film thickness of H-alone wafers is about 2210.8 Å. For all co-implanted cases, the wafers are inclined to split at a deeper position. The transferred thickness of S30 is about 2230 Å. For higher He^+ implantation energies, the thicknesses of the transferred Si layers are in the range of 2260–2270 Å. The relative thickness variation trend of H-alone, S30 and S45 is basically consistent with Ref. [3].

Figure 2 shows the H and He depth distribution profiles measured by SIMS before and after annealing. In Fig. 2(a), the dashed line shows the nominal H depth distribution calculated by SRIM for 18 keV. A vertical cyan dashed line also calculated by SRIM is plotted at the location of the damage peak. The solid lines present the as-implanted H distributions of H-alone, S30 and S45, respectively. The concentration peaks of H-alone, S30 and S40 are located around 2080 Å. Regardless of the implantation conditions, the peak of the H profiles simulated by SRIM is located slightly shallower than the data measured by SIMS.

Figure 2(b) shows the H distributions of H-alone, S30 and S45 after annealing at 500℃ for 30 min measured by SIMS. After the annealing, the concentration peak of H-alone wafer is located around 2166 Å. For the co-implanted samples, they are located around 2233 Å, 2249 Å for S30 and S45, respectively. It should be mentioned that the locations of these peaks are very close to the actual splitting positions. The previous works have mentioned a key feature of H evolution, namely a narrowing phenomenon of the concentration distribution under annealing, with the loss occurring mostly on the shallow side.[16–18] After annealing, all the samples exhibit the narrowing phenomenon around the position of maximum concentration peak. In addition, S45 presents the most remarkable H concentration narrowing phenomenon, which may be responsible for the best thickness uniformity obtained among the three implantation conditions.

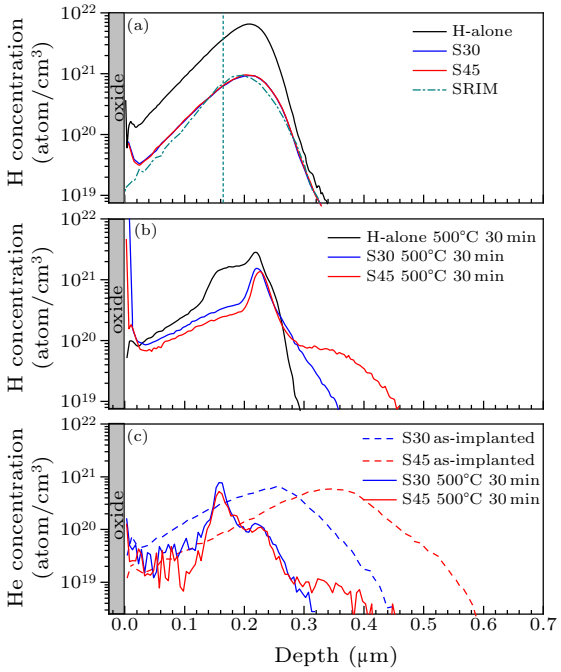

Fig. 2. [(a), (b)] H and (c) He depth distributions calculated by SRIM and measured by SIMS before and after annealing.

The He profiles of S30 and S45 before and after annealing are shown in Fig. 2(c). It is clearly observed that He distribution of S30 has a large overlap with the H profile, while the He profile is much deeper than the H profile for S45. It is reported that He would be captured at the locations of damage and concentration peeks of H for the co-implanted samples with shallower He distribution than H.[12] In our study, the redistribution of He towards to H-implantation induced defects is also observed. In addition to the primary concentration peaks, the secondary peaks of He concentration are located around 2176 Å, 2279 Å for S30 and S45, respectively. Hence, according to Figs. 1(b), 2(b) and 2(c), it can be concluded that the splitting position of a co-implanted sample occurs around where H

maximum concentration peak overlaps with the secondary peak of He concentration after annealing.

Figure 3 shows the XTEM images of platelets, micro-cracks, damage layers of the sample wafers after annealing 500℃ for 30 min. For the H-alone sample, the widest damage zone can be seen in Fig. 3(a). The defective layer with a width of 155 nm starts at a depth of about 140 nm from the Si/SiO_2 interface. For both S30 and S45, the defective layer is located at about 205 nm underneath the Si/SiO_2 interface. However, the width of the defect zone is 127 nm when the He distribution overlaps with the H profile (S30), and it reduces to 87 nm as He atoms distribute at the position located deeper than H profile (S45). The widest damage zone of H-alone is mainly due to the larger implantation dose. For the co-implantation samples, when the He profile largely overlaps with H, the higher amount of implantation damage would be generated.[3] Hence, S45 achieves the narrowest one. In addition, concomitant with the reduced defect zone, the micro-cracks in S45 are not as severe as those in the H-alone and S30 samples, thus yielding the transferred film with improved thickness uniformity.

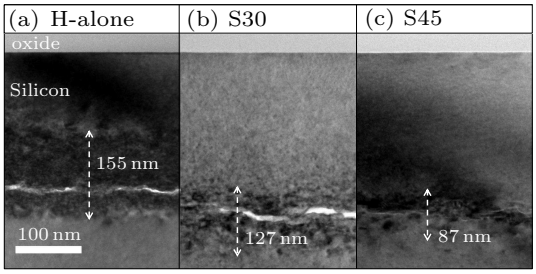

Fig. 3. XTEM micrographs for the samples after annealing at 500℃ for 30 min: (a) H-alone, (b) S30, and (c) S45.

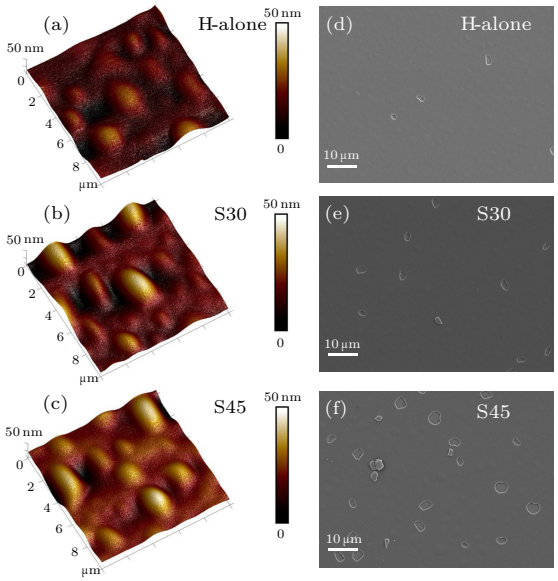

Fig. 4. Plan view images of the H-alone S30 and S45 samples after annealing at 500℃ for 30 min. [(a), (b) and (c)] 3D AFM images, [(d), (e) and (f)] SEM images.

During annealing, the platelets grow up by Ostwald ripening and then coalesce to form nano- and micro-cracks. These cracks would eventually split the top silicon film when the implanted surfaces are bonded to stiffeners. If the implanted wafer is not bonded, the blisters would appear on the surface due to the pressure inside the platelets and micro-cracks. Therefore, the ion-slicing process is often optimized by the study of blistering phenomena at free surfaces of implanted wafer without the time-consuming bonding process.

Figure 4 shows the plan view images obtained by AFM and SEM of the H-alone and co-implanted samples after annealing at 500℃ for 30 min. The AFM images reflect the 3D morphology of the surface blistering, and the SEM pictures present the craters distributed on the sample surface. Under all these conditions, the blisters have an average diameter of about 2 μm (varying from 0.8 μm to 3 μm). However, their maximum heights reach up to about 27 nm, 39 nm and 47 nm for H-alone, S30 and S45, respectively. From the comparison of the SEM images, it is obvious that both size and density of craters on S45 are much larger than those on H-alone and S30, which implies that the most efficient splitting is achieved in S45.

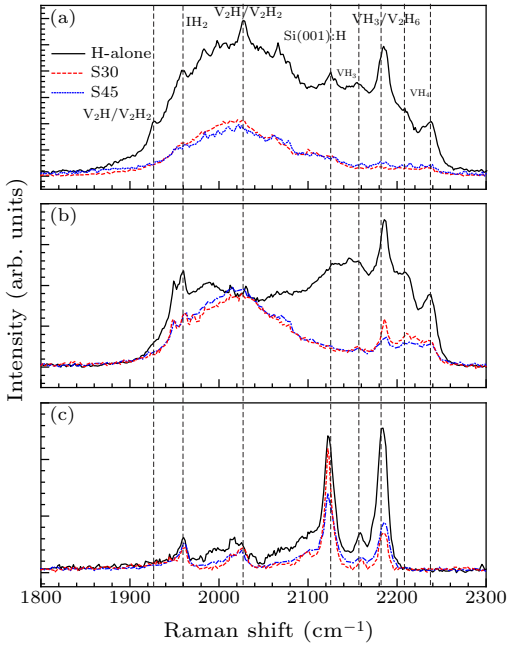

Fig. 5. Raman spectra of H-alone, S30 and S45 specimens (a) after implantation, (b) after annealing at 300℃ for 3 min, and (c) after annealing at 500℃ for 30 min.

Due to the fact that He would diffuse toward platelets and micro-cracks to pressurize the cavities and eventually form blisters, the difference of blistering behaviors between S30 and S45 is attributed to the proportion of He implantation dose which could contribute to pressurization. Compared with the cases whose He depth is shallower than H, a higher blistering efficiency could be achieved when the He profile is located underneath the H profile without overlap.[12] As shown in Fig. 2, compared with S45, a larger portion of He in S30 is located at shallower depth than the H maximum concentration peak. For this portion of He, they would be more readily trapped around

the maximum damage induced by H implantation and contribute less to the pressurization process located at the position of the H concentration peak. Hence, compared to S30, He atoms in S45 participate in the pressurization process more efficiently, which will be further validated by Raman spectra shown in Fig. 5.

Figure 5 shows the Raman spectra obtained on the H-alone, S30 and S45 specimens. Several main characteristic peaks assigned to the hydrogenated complexes are indicated by the dashed lines in Fig. 5(a).[18–20] The characteristic signatures in the low frequency region (LF mode, $\lambda < 2050\,\mathrm{cm}^{-1}$) correspond to multi-vacancy hydrogenated complexes (V_nH_m, $n \geq m$) and hydrogen-saturated self-interstitial complexes (IH_2). Those in the high frequency range (HF mode, $\lambda > 2050\,\mathrm{cm}^{-1}$) are predominantly due to the multi-hydrogen complexes (e.g., VH_3, VH_4 and V_2H_6). During the annealing process, the hydrogenated complexes will transit from the LF mode and IH_2 to the HF mode.[11] The multi-hydrogen complexes (e.g., VH_3, VH_4 and V_2H_6) belonging to the HF mode are proved to be the precursors for the platelets.[21] As the annealing process is extended, the platelets and micro-cracks will be formed, as the appearance of peaks around $2125\,\mathrm{cm}^{-1}$, i.e., a characteristic of (001) Si-H identified as the internal surfaces of platelets and micro-cracks.

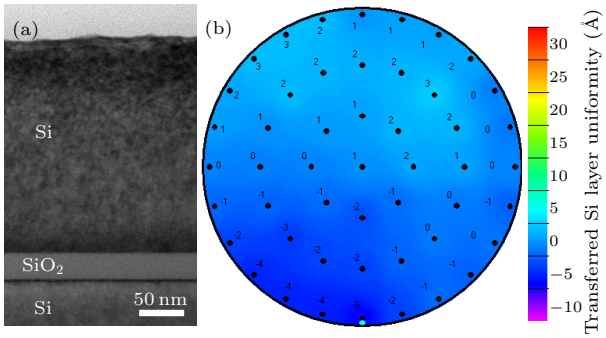

Fig. 6. Characterization of the fabricated SOI structure after the splitting process: (a) cross-sectional TEM image, and (b) 49-point mapping of the transferred Si layer thickness uniformity of S45.

For the as-implanted Si, plenty of vacancies and interstitials induced by implantation would trap H atoms to form hydrogenated complexes, and the majority of hydrogenated complexes corresponds to LF mode and IH_2, as shown in Fig. 5(a). Compared to the co-implanted specimens, the characteristic peak signals of HF mode are also observed in the H-alone sample, which could be attributed to the higher H implantation dose.[11–13] After annealing at 300℃ for 3 min, the peaks corresponding to LF mode in the H-alone sample decrease remarkably. For the co-implantation specimens, this thermal process leads to the appearance of the characteristic peak in HF mode and the peak amplitude of VH_3/V_2H_6 of S45 is higher than that of S30, as observed in Fig. 5(b). As the annealing process in performed at 500℃ for 30 min, the characteristic peaks of LF mode almost disappear for all the samples, while the multi-hydrogen complexes related HF mode and (001) Si-H characteristic peak emerge (Fig. 5(c)). In addition, the characteristic peak intensity of (001) Si–H for S45 is comparable to the H-alone specimen, but much higher than S30, which may interpret the high efficiency of He atoms in S45 in terms of blistering behavior.

According to the comprehensive consideration of the influences of co-implantation on the blistering and the top Si uniformity after splitting, the implantation condition for S45 has been chosen for SOI fabrication. Figure 6(a) is an XTEM image of the as-split SOI structure. The mean thickness of the transferred Si layer is about 2263 Å and its thickness uniformity is 8.55 Å, which are measured by 49 points SE, as described in Fig. 6(b). This result satisfies the demand for the subsequent fabrication of FD-SOI.

In summary, an efficient approach for highly uniform top Si layer transfer has been demonstrated by H/He co-implantation. When the He profile is deeper than H, He can participate in the Si layer transfer process more efficiently, and the transferred Si layer has better uniformity. For the H/He co-implantation, the splitting occurs around the position where the maximum concentration peak of H overlaps the secondary concentration peak of He after annealing. In the SOI manufacture, our process may provide an approach for the exploitation of efficient solution to fabricate FD-SOI wafers with highly thickness uniformity.

References

[1] Bruel M 1995 *Electron. Lett.* **31** 1201
[2] Grisolia J et al 2000 *Appl. Phys. Lett.* **76** 852
[3] Nguyen P et al 2005 *J. Appl. Phys.* **97** 083527
[4] Agarwal A et al 1998 *Appl. Phys. Lett.* **72** 1086
[5] Weldon M K, Collot M, Chabal Y J et al 1998 *Appl. Phys. Lett.* **73** 3721
[6] Huang L, Tong Q, Chao Y et al 1999 *Appl. Phys. Lett.* **74** 982
[7] Aspar B, Bruel M, Moriceau H et al 1997 *Microelectron. Eng.* **36** 233
[8] Reboh S, Schaurich F, Declemy A et al 2010 *J. Appl. Phys.* **108** 023502
[9] Moutanabbir O, Terreault B, Chicoine M et al 2007 *Phys. Rev. B* **75** 075201
[10] Nguyen P, Bourdelle K K, Maurice T et al 2007 *J. Appl. Phys.* **101** 033506
[11] Daghbouj N, Cherkashin N, Darras F X et al 2016 *J. Appl. Phys.* **119** 135308
[12] Cherkashin N, Daghbouj N, Seine G et al 2018 *J. Appl. Phys.* **123** 161556
[13] Cherkashin N, Daghbouj N, Darras F X et al 2015 *J. Appl. Phys.* **118** 245301
[14] Schwarzenbach W, Cauchy X, Bonnin O et al 2011 *ECS Trans.* **35** 239
[15] Ziegler J F and Biersack J P, See http://www.srim.org for SRIM computer code
[16] Bedell S W and Lanford W A 2001 *J. Appl. Phys.* **90** 1138
[17] Höchbauer T F, Misra A et al 2006 *Nucl. Instrum. Methods Phys. Res.* **242** 623
[18] Terreault B 2007 *Phys. Status Solidi A* **204** 2129
[19] Moutanabbir O, Terreault B, Chicoine M et al 2005 *Appl. Phys. A* **80** 1455
[20] Moutanabbir O and Terreault B 2005 *Appl. Phys. Lett.* **86** 051906
[21] Personnic S, Bourdelle K K, Letertre F et al 2008 *J. Appl. Phys.* **103** 023508